J. metamorphic Geol., 2006, **24,** 591–602 doi:10.1111/j.1525-1314.2006.00656.x

Mineral isograds and metamorphic zones of the Anglesey blueschist belt, UK: implications for the metamorphic development of a Neoproterozoic subduction–accretion complex

T. KAWAI,[1] B. F. WINDLEY,[2] M. TERABAYASHI,[3] H. YAMAMOTO,[4] S. MARUYAMA[1] AND Y. ISOZAKI[5]
[1]*Department of Earth and Planetary Sciences, Tokyo Institute of Technology, O-okayama 2-12-1, Meguro, Tokyo 152-8551, Japan (tkawai@geo.titech.ac.jp)*
[2]*Department of Geology, University of Leicester, Leicester LE1 7RH, UK*
[3]*Department of Safety Systems Construction Engineering, Kagawa University, Kagawa 761-0396, Japan*
[4]*Department of Earth and Environmental Sciences, Kagoshima University, Kagoshima 890-0065, Japan*
[5]*Department of Earth Science & Astronomy, Graduate School of Arts and Sciences, The University of Tokyo 3-8-1 Komaba, Meguro Tokyo 153-8902, Japan*

ABSTRACT The 560–550 Ma blueschists and associated rocks in Anglesey, UK were derived from a subduction–accretion complex. The blueschist unit is divided into three mineral zones by two newly mapped metamorphic isograds; zone I sub-greenschist facies, (crossite isograd), zone II blueschist facies, (barroisite isograd), zone III epidote-amphibolite facies. The zones and isograds dip gently to the east, and decrease in metamorphic grade from the central high-pressure zone III to lower grade zones II and I to the west and east. The *P–T* conditions estimated from zoned amphibole indicate an anticlockwise *P–T* path following adjustment to a cold geotherm. This path is well preserved in the compositional zoning of Na–Ca amphibole that have a core of barroisite surrounded by a rim of crossite, although this is only locally developed. The sense of subduction was to the east and exhumation to the west, as indicated by the metamorphic isograds. The symmetrical arrangement of the metamorphic zones with the deepest high-pressure rocks in the middle suggests an isoclinal antiformal structure that formed by wedge extrusion during exhumation in the subduction zone.

Key words: Anglesey; blueschist; mineral zones; *P–T* path.

INTRODUCTION

Blueschists are the exhumed products of subducted supracrustal rocks originally deposited in a trench and portion of the oceanic lithosphere. The subduction transports the material to the stability field of glaucophane along a cold geotherm (Ernst, 1963; Carman & Gilbert, 1983; Miyashiro, 1994). Generally, exhumation during wedge extrusion is thought to carry these high-pressure (HP) metamorphic rocks up and over a low-grade accretionary complex to form a sandwich structure (Maruyama *et al.*, 1996). Study of the metamorphic parameters of such blueschists enables the definition of metamorphic isograds and zones, which additionally provides information on structural-tectonic relations such as subduction polarity. Moreover, the mineral isograds, mineral chemistry, and textural evolution monitor the changing *P–T* conditions with time and the compositional characteristics in relation to XCO_2-H_2O provide key information on subduction tectonics. Comparative data are provided from blueschists in Anglesey, Wales, UK, and the mineralogy, metamorphic assemblages, metamorphic facies and facies series, and the *P–T* path of rocks in the blueschist belt are described.

GEOLOGICAL BACKGROUND

Glaucophane-bearing rocks occur in a NE-SW trending strip (about 28 km long and up to 6 km wide) of amphibolitic, micaceous and chloritic schists in eastern Anglesey, Wales, UK (Fig. 1). The glaucophane-bearing rocks have $^{40}Ar/^{39}Ar$ white-mica ages of 560–550 Ma (barroisite/crossite-rich concentrates) and 580–590 Ma (actinolite-rich concentrates) (Dallmeyer & Gibbons, 1987). Studies of these and associated rocks in Anglesey are numerous. Henslow (1822) first mapped the belt of 'chloritic schists', and thus defined the tectonic framework in which the blueschists occur, Blake (1888) discovered the glaucophane, and Greenly (1919) mapped and documented the geology of Anglesey putting the South Stack Group at the stratigraphic top. Later, Wood (1974) put the blueschists into the framework of an accretionary orogen containing mélanges and ophiolitic relicts, and made comparison with rocks in California. Shackleton (1969, 1975) in re-evaluating the Anglesey stratigraphy with way-up criteria reversed Greenly's stratigraphy putting the South Stack Group at the bottom, but regarded the Groups above to be in normal stratigraphic order, whereas Barber & Max (1979)

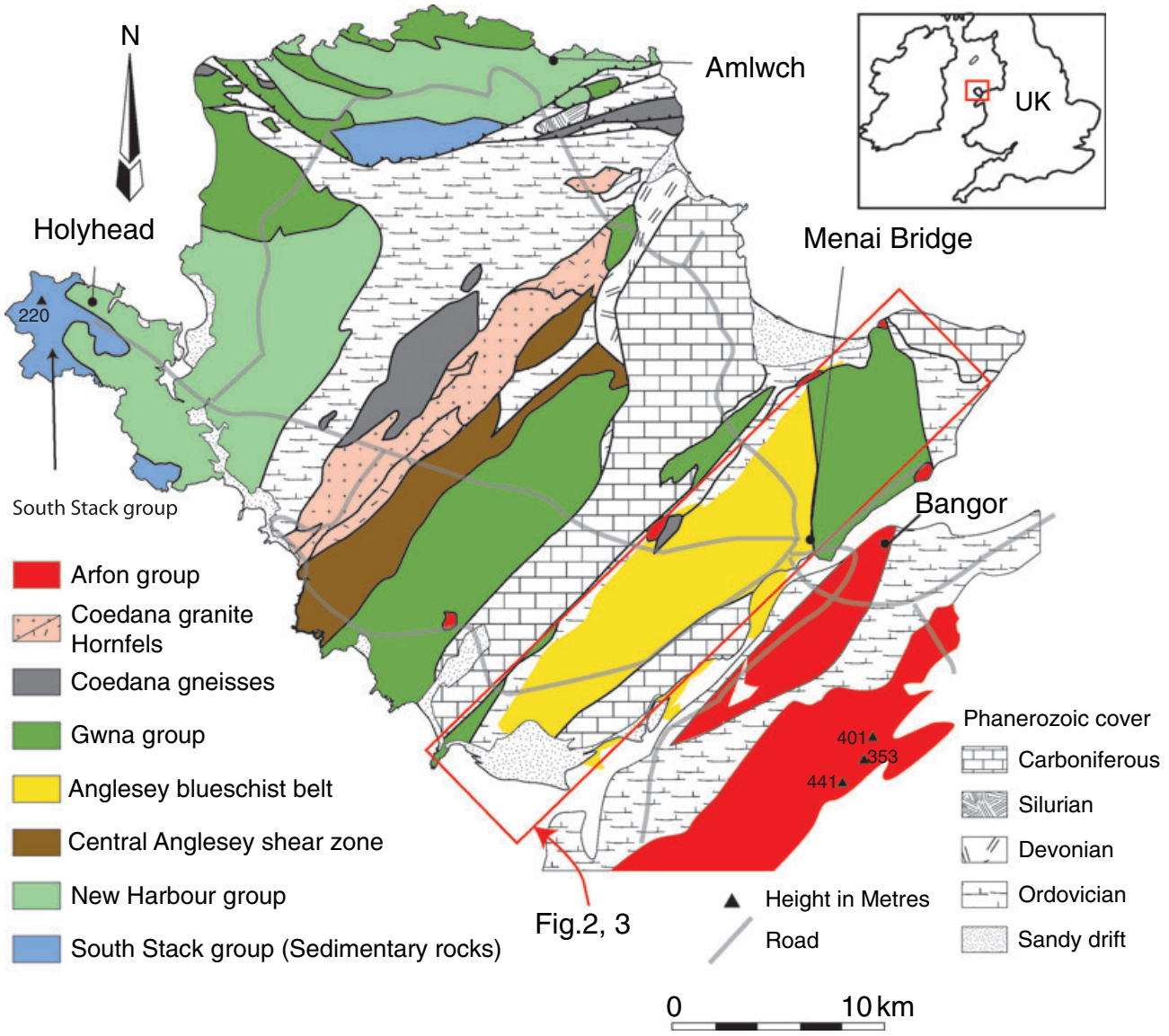

Fig. 1. Geological map of Anglesey island (adapted from Greenly, 1919 and Shackleton, 1969).

reassessed the tectonic stratigraphy, in particular proposing that the less deformed South Stack Group was thrust beneath the more highly deformed New Harbour Group. Gibbons (1983) suggested that the evidence in Anglesey for palaeo-subduction including the blueschists was weak, and Gibbons (1989) interpreted the tectonic belts in Anglesey in terms of suspect terranes. Gibbons & Mann (1983) first reported lawsonite in mafic blueschists, and Horák & Gibbons (1986) reclassified the blueschist amphibole in particular as crossite and barroisite. Gibbons & Gyopari (1986) proposed an anticlockwise *P–T* trajectory for the blueschists formed as a result of the subduction of oceanic crust, and Gibbons & Horák (1990) interpreted the contiguous, fault-bounded metamorphic belts as suspect terranes on the margin of Avalonia.

However, in spite of all these studies, the Anglesey blueschists have never been interpreted in the light of a modern understanding of comparative blueschist belts in Pacific-type accretionary orogens such as Japan and California. Therefore, their role in the geotectonic development on the subducting continental margin has never been fully appreciated.

GEOLOGICAL OUTLINE

In Anglesey (Fig. 1) several schist belts, ranging in metamorphic grade from zeolite or prehnite-pumpellyite to blueschist, contain comparative lithologies such as metamorphosed pillow basalts, some of which have MORB-type geochemistry (Thorpe, 1993), that are now mostly greenschists and blueschists, together

with sandstones, shales and limestones. The Anglesey blueschists and related rocks have the same characteristics as those of modern analogues in Pacific-type or B-type (Benioff zone) orogens (Maruyama *et al.*, 1996). As shown by the geological map of Anglesey (British Geological Survey, 1980) the central blueschist belt contains mica schists, hornblende schists and glaucophane schists, minor quartz schists and limestones. To the north-east and north-west of the blueschist belt, the Gwna Group comprises greenschists, spilitic lavas and diabases, rare glaucophane schists, and minor quartzities and limestones (Fig. 2). From a comparison of the lithologies and from our metamophic studies, it is considered that the blueschists and the Gwna Group are parts of the same volcano-sedimentary unit, the main difference being that the Gwna Group on the whole has a lower metamorphic grade, from which it is inferred that the central blueschist belt was more deeply subducted. These two units were recrystallized at different P–T conditions but along a single subduction zone geotherm, as described below.

The NE-trending belt of greenschists and blueschists is bound on both sides by high-angle, NE-trending faults that are considered to be secondary faults. For example, in the largest outcrop of blueschists the schistosity is horizontal and clearly cut by bounding NE-trending secondary faults (Fig. 2). The fault between metamorphic zones II and III taken from the geological map (British Geological Survey, 1980), but lack of exposure makes it difficult to confirm in the field.

METHODS OF INVESTIGATION

During three summers mapping (2003–2005), 250 samples were collected, from which 80 thin sections of metabasites were examined carefully to delineate metamorphic isograds. Representative rock-forming minerals were analysed with a JEOL JXA8800 electron microprobe analyzer at the Department of Earth and Planetary Sciences, Tokyo Institute of Technology. Analytical conditions were: an accelerating voltage of 15 kV; a specimen current of 12 nA on a Faraday cup; a beam diameter of 1–5 μm; X-ray intensities were reduced using a ZAF matrix correction scheme. Representative analyses of major minerals are listed in Table 1.

Mineral abbreviations follow Kretz (1983); additional minerals are: Ames (amesite); Arg (aragonite); Brs (barroisite); Clin (clinochlore); Crs (crossite); Fgln (ferro-glaucophane); Ph (phengite); Win (winchite).

METAMORPHIC ZONATION

Mineral assemblages in mafic schists are divisible into three zones: I (epidote-chlorite), II (crossite-epidote), III (barroisite-epidote) (Figs 3 & 4). For our use of the term crossite, see discussion on amphibole below.

Zone I metabasites contain the common mineral assemblage calcite-chlorite-epidote, in addition to excess phases; albite, quartz, titanite, phengitic mica and

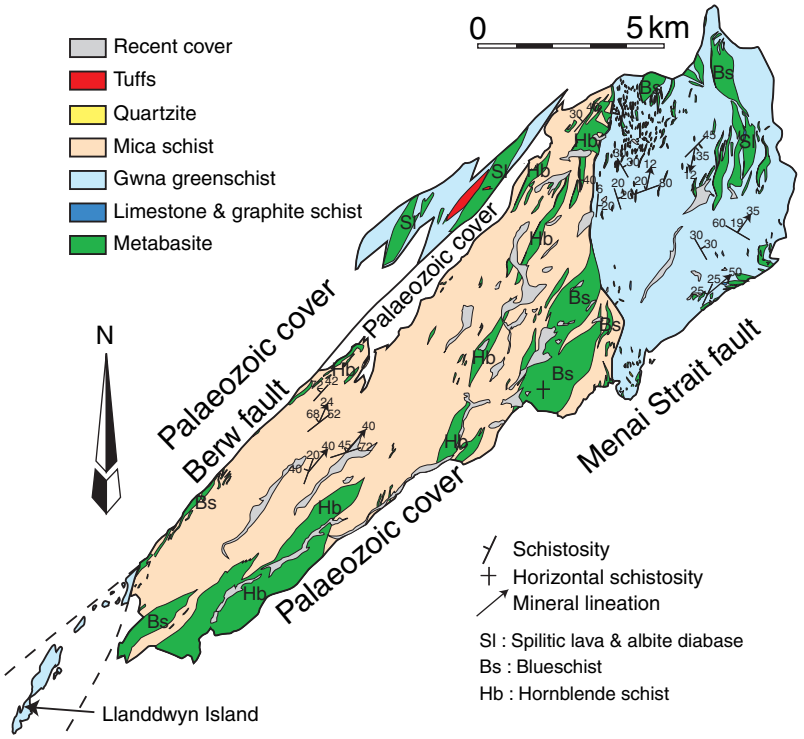

Fig. 2. (a) Geological map of east Anglesey schist belt (British Geological Survey, 1980); (b) Geological map of Llanddona area (British Geological Survey, 1980).

Table 1. Representative chemical composition of epidote, chlorite, phengite and Na-Ca amphibole in metabasites.

	Zone I					Zone II										
Sample No.	A519		A591			A554			A587				AMW145			
Mineral	Ep	Chl	Ep	Chl	Ph	Ep	Chl	Crs	Ep	Chl	Crs	Ph	Ep (core)	Ep (rim)	Chl	Crs
SiO_2	37.34	27.06	37.77	27.16	52.25	38.31	29.87	52.90	38.32	28.91	57.41	47.20	37.83	38.42	29.16	56.41
TiO_2	0.10	0.03	0.05	0.09	0.00	0.10	0.05	0.00	0.15	0.03	0.02	0.20	0.01	0.05	0.00	0.18
Al_2O_3	21.81	18.65	21.71	19.65	23.77	23.58	17.45	10.10	23.07	17.61	8.90	26.46	23.03	23.70	17.66	8.86
Cr_2O_3	0.00	0.00	0.00	0.00	0.00	0.00	0.00	0.00	0.00	0.00	0.00	0.00	0.00	0.00	0.00	0.00
Fe_2O_3	15.73	0.00	15.30	0.00	2.46	13.71	0.00	4.05	13.57	0.00	2.71	2.75	15.40	13.96	0.00	2.26
FeO	0.00	26.43	0.00	24.66	3.12	0.00	21.28	12.16	0.00	20.78	11.88	2.45	0.00	0.00	22.45	14.05
MnO	0.32	0.63	0.23	0.45	0.02	0.27	0.34	0.20	0.34	0.38	0.17	0.03	0.35	0.36	0.53	0.19
MgO	0.03	14.31	0.00	16.82	4.00	0.03	17.85	10.80	0.02	18.30	9.30	2.63	0.04	0.00	17.71	8.27
CaO	22.34	0.18	22.98	0.11	0.06	23.11	0.17	1.90	22.70	0.12	0.90	0.11	22.87	23.07	0.16	1.43
Na_2O	0.00	0.00	0.00	0.02	0.06	0.02	0.23	5.30	0.01	0.06	6.41	0.49	0.02	0.02	0.05	6.64
K_2O	0.01	0.06	0.03	0.06	10.85	0.04	0.22	0.10	0.03	0.03	0.04	9.83	0.01	0.02	0.06	0.05
Totals	97.68	87.35	98.07	89.02	96.60	99.16	87.46	97.51	98.20	86.22	97.73	92.19	99.57	99.59	87.78	98.35
Oxygen	12.5	14	12.5	14	11	12.5	14	23	12.5	14	23	11	12.5	12.5	14	23
Si	3.003	2.884	3.024	2.807	3.484	3.011	3.077	7.515	3.039	3.016	8.013	3.297	2.980	3.008	3.015	7.933
Ti	0.006	0.003	0.003	0.007	0.000	0.006	0.004	0.000	0.009	0.002	0.002	0.011	0.001	0.003	0.000	0.020
Al	2.068	2.344	2.049	2.394	1.869	2.185	2.119	1.692	2.157	2.166	1.464	2.179	2.139	2.188	2.152	1.469
Cr	0.000	0.000	0.000	0.000	0.000	0.000	0.000	0.000	0.000	0.000	0.000	0.000	0.000	0.000	0.000	0.000
Fe^{3+}	0.952	0.000	0.922	0.000	0.124	0.811	0.000	0.433	0.810	0.000	0.284	0.145	0.913	0.823	0.000	0.239
Fe^{2+}	0.000	2.356	0.000	2.132	0.174	0.000	1.833	1.445	0.000	1.813	1.386	0.143	0.000	0.000	1.941	1.653
Mn	0.022	0.057	0.015	0.040	0.001	0.018	0.029	0.024	0.023	0.033	0.020	0.002	0.023	0.024	0.046	0.022
Mg	0.004	2.273	0.000	2.591	0.398	0.003	2.740	2.287	0.002	2.845	1.934	0.273	0.005	0.000	2.729	1.733
Ca	1.925	0.020	1.972	0.012	0.004	1.946	0.019	0.289	1.929	0.014	0.135	0.008	1.930	1.936	0.018	0.215
Na	0.000	0.000	0.000	0.004	0.008	0.002	0.046	1.460	0.001	0.012	1.736	0.067	0.003	0.003	0.010	1.811
K	0.001	0.008	0.003	0.007	0.924	0.004	0.029	0.018	0.003	0.004	0.007	0.877	0.001	0.002	0.008	0.009

	Zone III															
Sample No.	A650				A747						A770		A719			
Mineral	Ep	Chl	Brs (core)	Crs (rim)	Ep	Chl	Brs	Win	Gln	Ph	Ep	Brs	Ep	Chl	Act	Brs
SiO_2	38.50	28.35	50.80	56.94	37.84	27.55	49.58	53.18	56.20	49.71	38.28	51.98	38.59	28.35	54.67	51.36
TiO_2	0.09	0.02	0.10	0.03	0.08	0.07	0.20	0.09	0.02	0.07	0.06	0.12	0.13	0.02	0.07	0.17
Al_2O_3	23.94	18.57	7.70	8.26	23.12	18.78	9.22	5.44	8.65	24.38	23.09	6.33	26.77	18.57	1.75	6.81
Cr_2O_3	0.00	0.00	0.00	0.00	0.00	0.00	0.00	0.00	0.00	0.00	0.00	0.00	0.00	0.00	0.00	0.00
Fe_2O_3	13.31	0.00	3.26	3.47	14.06	0.00	2.81	2.67	2.01	0.00	13.29	1.96	9.01	0.00	0.29	2.08
FeO	0.00	22.36	13.47	11.95	0.00	24.98	14.73	14.12	13.98	3.98	0.00	11.18	0.00	22.36	12.24	9.49
MnO	0.23	0.49	0.20	0.18	0.33	0.59	0.36	0.32	0.17	0.00	0.14	0.29	0.20	0.49	0.26	0.17
MgO	0.03	17.60	10.90	8.40	0.01	15.72	9.43	11.06	8.49	2.84	0.01	13.38	0.20	17.60	15.54	15.23
CaO	23.11	0.10	7.30	1.39	22.70	0.11	6.47	7.06	1.36	0.04	22.58	9.17	23.23	0.10	12.09	11.60
Na_2O	0.03	0.04	3.50	6.05	0.01	0.04	4.33	3.38	6.24	0.49	0.00	2.53	0.02	0.04	0.39	1.10
K_2O	0.02	0.05	0.30	0.05	0.02	0.04	0.25	0.13	0.05	10.18	0.03	0.13	0.00	0.05	0.06	0.14
Totals	99.26	87.57	97.53	96.71	98.17	87.89	98.37	97.45	97.18	91.71	97.49	97.07	98.15	87.57	97.35	98.15
Oxygen	12.5	14	23	23	12.5	14	23	23	23	11	12.5	23	12.5	14	23	23
Si	3.017	2.938	7.389	8.060	3.009	2.891	7.216	7.712	7.977	3.478	3.051	7.498	3.010	2.938	7.866	7.304
Ti	0.005	0.002	0.011	0.003	0.005	0.006	0.022	0.010	0.002	0.004	0.004	0.013	0.008	0.002	0.008	0.018
Al	2.211	2.269	1.320	1.378	2.167	2.323	1.582	0.929	1.448	2.011	2.170	1.077	2.462	2.269	0.297	1.142
Cr	0.000	0.000	0.000	0.000	0.000	0.000	0.000	0.000	0.000	0.000	0.000	0.000	0.000	0.000	0.000	0.000
Fe^{3+}	0.785	0.000	0.357	0.369	0.841	0.000	0.417	0.291	0.215	0.000	0.797	0.213	0.529	0.000	0.031	0.223
Fe^{2+}	0.000	1.938	1.638	1.415	0.000	2.192	1.793	1.712	1.659	0.233	0.000	1.348	0.000	1.938	1.473	1.129
Mn	0.016	0.043	0.025	0.021	0.022	0.053	0.044	0.039	0.021	0.000	0.010	0.035	0.013	0.043	0.031	0.021
Mg	0.003	2.718	2.363	1.771	0.002	2.458	2.046	2.390	1.797	0.297	0.001	2.876	0.023	2.718	3.332	3.228
Ca	1.940	0.011	1.138	0.211	1.934	0.013	1.009	1.097	0.207	0.003	1.928	1.417	1.941	0.011	1.864	1.768
Na	0.004	0.007	0.987	1.661	0.001	0.009	1.221	0.951	1.716	0.067	0.000	0.708	0.003	0.007	0.107	0.304
K	0.002	0.006	0.056	0.010	0.002	0.006	0.046	0.025	0.009	0.910	0.003	0.025	0.000	0.006	0.011	0.025

presumably H_2O-rich fluid. Carbonate is calcite and aragonite has not been identified.

Zone II mafic schists yield the mineral assemblage epidote-chlorite-crossite with the excess phases; albite, quartz, titanite, phengitic mica and presumably H_2O-rich fluid. Gibbons & Mann (1983) reported that lawsonite occurs in four localities; one is in zone II, and three are in zone III. The lawsonite-bearing samples are insufficiently widespread to draw a lawsonite isograd (Fig. 3), and we do not know whether the lawsonite might have formed by fluid infiltration in the fault associated with the special pattern of these lawsonite occurrences.

Zone III metabasites contain epidote, chlorite and the Na-Ca amphibole of barroisite, crossite, actinolite and winchite; the zone is defined by the appearance of barroisite that consumes epidote, crossite and minor chlorite. The $^{40}Ar/^{39}Ar$ white-mica ages of 590–580 Ma

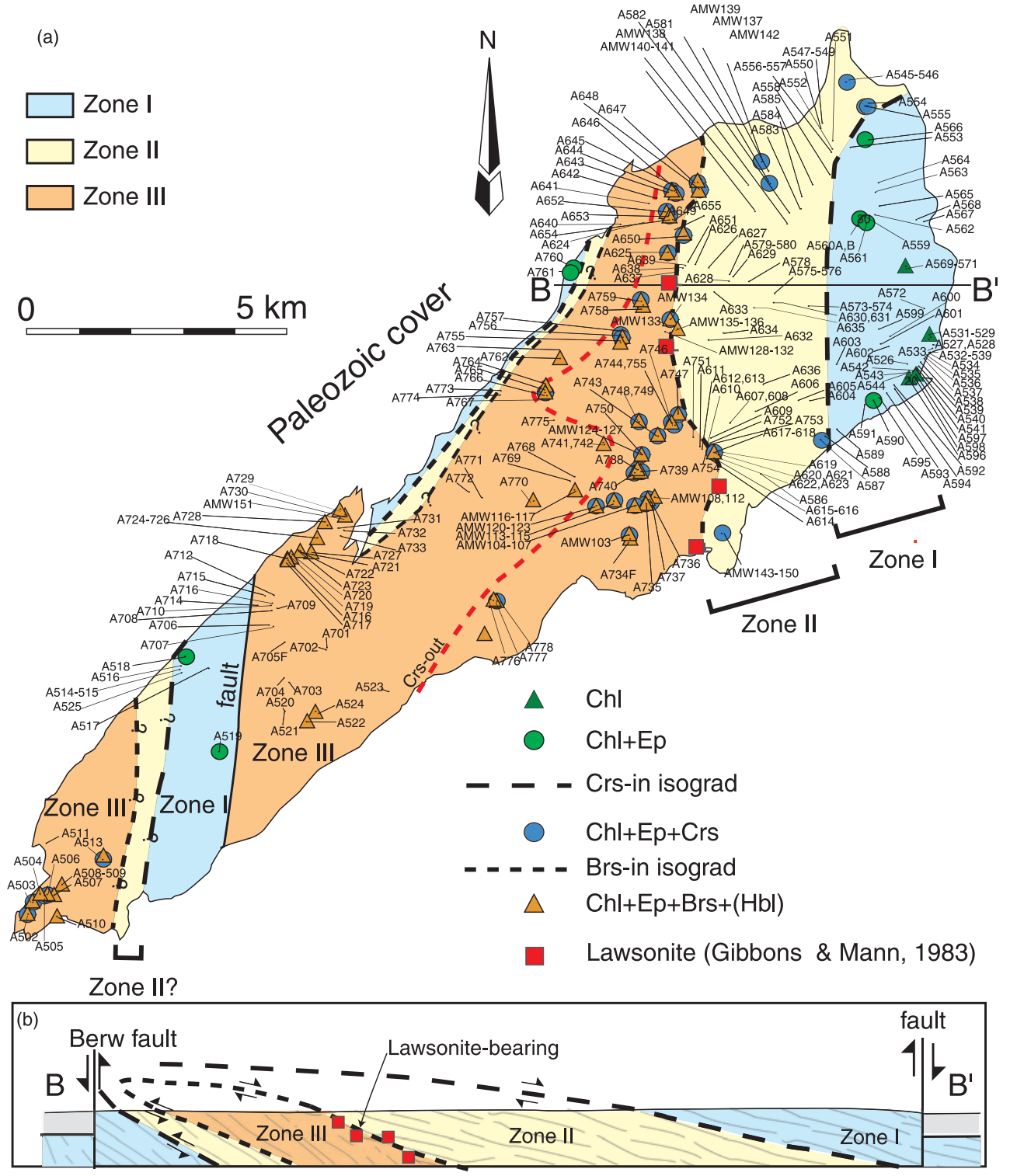

Fig. 3. (a) Sample localities and distribution of mineral assemblages in metabasites in three metamorphic zones; (b) Simplified cross-section along B-B′.

(actinolite-rich concentrates) suggest that the actinolite is possibly the relic of ocean-floor metamorphism (Dallmeyer & Gibbons, 1987). Thus, the actinolite has not been used for mineral zonation. Zone III equates to the Penmynydd metamorphic zone of the Anglesey map of the British Geological Survey (1980).

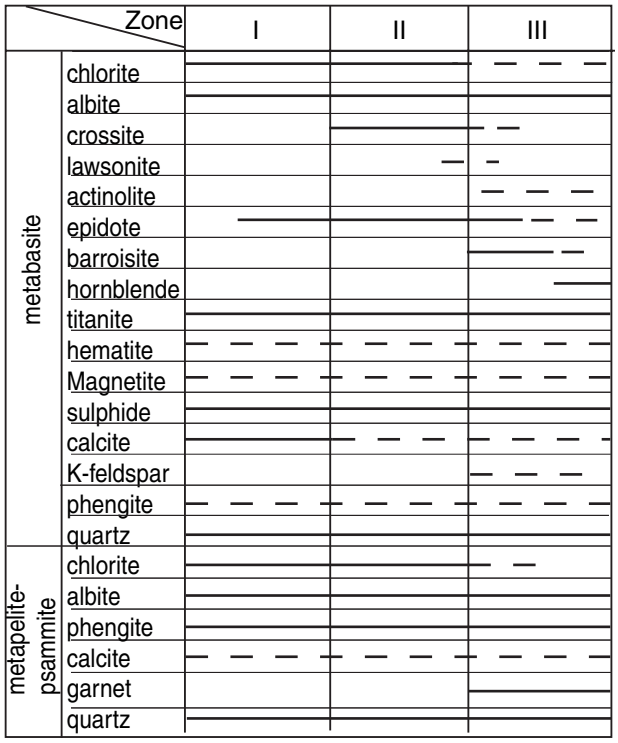

Fig. 4. The stable occurrence of minerals in metabasites and metapelite-psammites in the three zones. Solid line means major constituent and dashed line means minor constituent.

The spatial distribution of the mineral zones indicates a structurally downwards, westward increase of *P–T* towards a central high-*P–T* zone, followed by a structurally upwards decrease farther westward (Fig. 3).

OCCURRENCE, TEXTURES AND COMPOSITIONS OF METAMORPHIC MINERALS

We summarize the rock-forming mineralogy and textures used to calculate the *P–T* conditions, metamorphic reactions, and *P–T*-time path. Representative analyses of major rock-forming minerals are listed in Table 1.

Amphibole

Amphibole is most common in mafic schists of zones II and III and is almost tabular and has a preferred orientation; lengths are up to 0.1 mm in zone II and up to 0.5 mm in zone III.

Both sodic and calcic amphiboles were identified. Na-amphibole ranges in composition from magnesioriebeckite and crossite to glaucophane, whereas Ca–Na amphibole in zone III ranges widely from winchite, barroisite and hornblende to crossite (Fig. 5a). Zoning of Na-amphibole occurs in zone II, where crossitic amphibole is rimmed by magnesioriebeckite. Zoning of Ca–Na amphibole is common in zone III, where barroisitic amphibole is rimmed by crossite (Fig. 6), as recorded by Horák & Gibbons (1986). The term crossite was not used in the amphibole classification of Leake *et al.* (1997), but we prefer to retain it because crossite is pressure-dependent and usefully separates low-pressure riebeckite from high-pressure ferro-glaucophane, as in Fig. 5b. Thus, we follow Otsuki & Banno (1990) in Fig. 10 and Matsumoto *et al.* (2003).

The Fe^{3+} contents in amphibole were calculated as averages of maximum and minimum values for O = 23, using the computer program AX and the method of Holland & Blundy (1994). Chemical compositions of analysed amphibole are shown in Fig. 5a, where

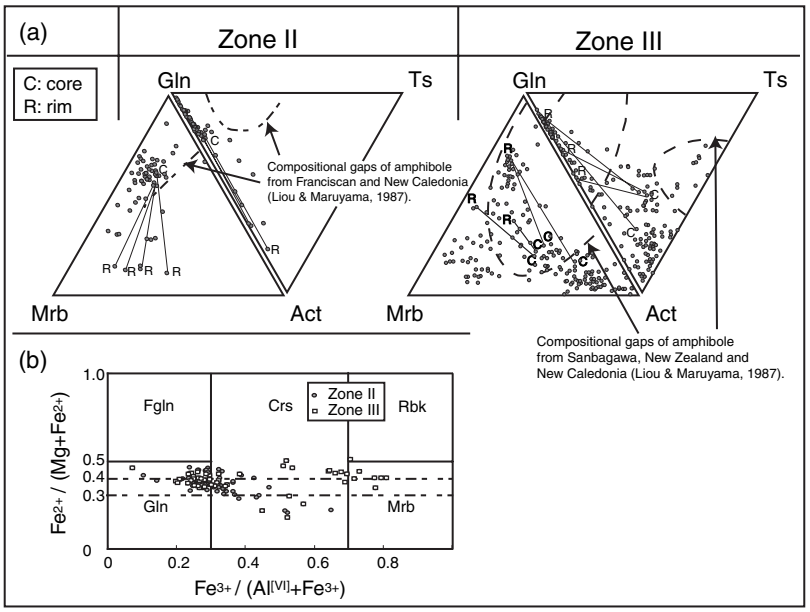

Fig. 5. (a) Compositional variations of Ca-Na amphibole from zones II and III in Anglesey expressed in the glaucophane-magnesioriebeckite-actinolite-tschermakite system. Tie-lines connect compositions of zoned amphibole. Compositional gaps are delineated after Liou & Maruyama (1987); (b) Compositional variations of Anglesey sodic amphibole from zones II and III metabasites on a Miyashiro diagram.

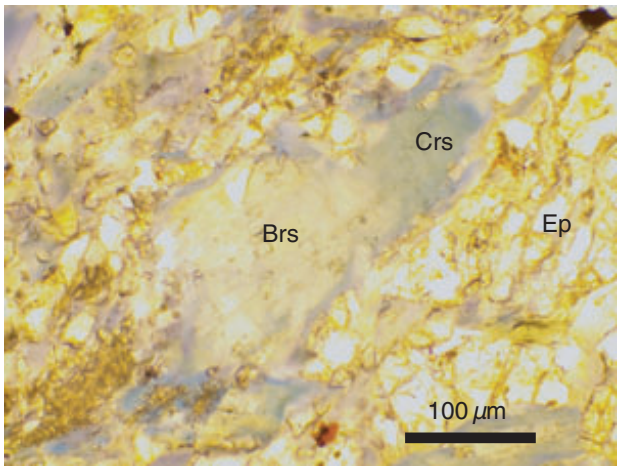

Fig. 6. Photomicrograph showing barroisitic amphibole rimmed by crossite in a metabasite from zone III.

glaucophane (Gln), magnesioriebeckite (Mrb), actinolite (Act) and tschermakite (Ts) components were calculated as $Al^{VI}/(Al^{VI} + Fe^{3+}) \times Na/(Ca + Na)[B]$, $Fe^{3+}/(Al^{VI} + Fe^{3+}) \times Na/(Ca + Na)[B]$, $(2\text{-}Al^{IV})/2 \times Ca(Ca + Na)[B]$ and $Al^{IV}/2 \times Ca/(Ca + Na)[B]$, respectively. Amounts of Al^{IV} by the edenite substitution ($(Na + K)_A Al^{IV} = [\,]_A Si$) are not distinguished from those by the tschermak substitution ($Al^{VI} Al^{IV} = MgSi$). Analysed amphibole has no compositional gaps. In comparison, there are compositional gaps in amphibole from New Caledonia, New Zealand and the Franciscan in California (Liou & Maruyama, 1987). The $Mg/(Mg + Fe^{2+})$ of amphibole is 0.53–0.98 (zone II) and 0.49–1.00 (zone III) and the $Fe^{3+}/(Fe^{3+} + Al)$ is 0.00–0.83 (zone II) and 0.00–1.00 (zone III). The Ti contents of amphibole are not observed.

The chemical compositions of analysed Na-amphibole are shown in Fig. 5b with the nomenclature after Miyashiro (1957). The X_{Fe2+} of Na-amphibole ranges from 0.21 to 0.46 in zone II and from 0.18 to 0.51 in zone III. In spite of a wide range of compositional scatter, the majority plot around 0.30 and 0.40 in zones II and III, respectively.

Epidote

Epidote occurs as a common metamorphic mineral in metabasites in zone II, and less commonly in zone III. It occurs commonly in the west of zone I, but it is absent in the east. Fine- to medium-sized crystals have an irregular or tabular shape. The orientations of the epidote are almost the same as those of amphibole and chlorite.

The X_{Fe3+} content of epidote is plotted against analysed samples in Fig. 7, in which the horizontal axis roughly corresponds to an increase of metamorphic grade from east to west. Analysed epidote contains low MnO (0.05–0.63 wt%) and TiO_2 and negligible amounts of Na_2O and MgO. At least five analyses were made in each polished section in which core and rim compositions were determined. Almost all analysed epidote has consistently higher X_{Fe3+} in the core than the rim, suggesting progressive growth with increasing temperature. The X_{Fe3+} ranges from 0.34 to 0.28 in zone I and becomes more aluminous from east to west. In zone II it reaches up to 0.23 and in zone III to 0.16.

Phengite

Phengitic mica occurs as a minor mineral in metabasites. It occurs as fine-grained oriented crystals, has a platy form and is aligned along the schistosity. The compositions of phengite are listed in Table 1. The muscovite components of phengite are lowest in zone I.

Lawsonite

Gibbons & Mann (1983) first reported lawsonite in the blueschist belt (Fig. 3). It is restricted to bands <1 m wide that are interleaved with basic crossite schists and muscovite-quartz schists. Coarse tabular lawsonite grains up to 2 mm long occur in a fine-grained matrix consisting of crossite, actinolite, chlorite, albite and quartz, and minor titanite, epidote, phengite and oxides. Some elongate lawsonite is parallel to the matrix foliation, but some tabular grains cross-cut the foliation and contain inclusions of glaucophane. Some lawsonite is broken by boudinage, the fractures are

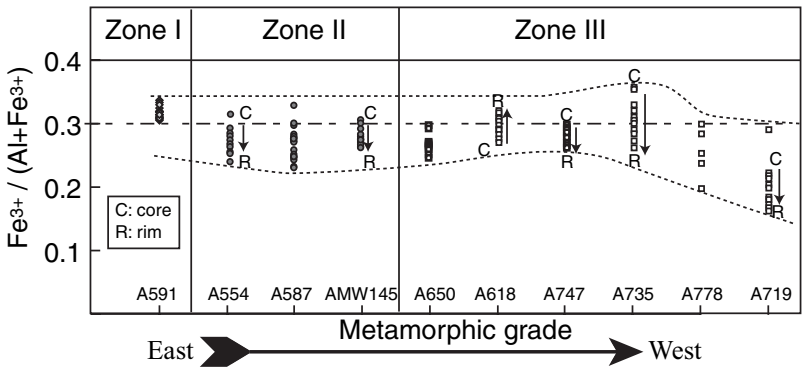

Fig. 7. Compositional ranges of epidote from the Anglesey blueschist belt. Both core and rim compositions are arranged according to their inferred metamorphic grade.

infilled with quartz, and some is altered to chlorite (Gibbons & Mann, 1983).

Chlorite

Chlorite is common in zones I and II and less common in zone III, reflecting the prograde reaction that consumes chlorite, epidote and albite to form crossite and barroisite. Chlorite is mostly pale green and tends to form a lineation on the rock schistosity. In zone III some chlorite appears as a retrograde mineral, fringing barroisitic amphibole and altering amphibole in lawsonite-bearing rocks adjacent to the fault with zone II (see Gibbons & Mann, 1983).

Compositions of analysed chlorite in metabasites are plotted in an Al-Fe*-Mg diagram in Fig. 8. Each zone contains large compositional variations in chlorite. The maximum Al contents are highest in zone III.

Other minerals

Garnet was not identified in metabasites, but it occurs in pelites in zone III. It is euhedral in form and about 5 mm in maximum diameter. The garnet typically has low Prp component ($Prp_{1.0-1.5}$, Alm_{33-38}, Grs_{31-35} and $Sps_{2.8-3.4}$).

Albite is ubiquitous in all zones; in zone III it occurs together, but rarely, with K-feldspar. Some albite is coarse-grained and exhibits cleavage and faint twinning; however most albite is free from twinning and cleavage. In zones I and II albite in metabasites has a nearly end-member composition of $X_{An} < 0.1$, but in zone III it ranges in composition from < 7 mol.% An and < 10 mol.% Or.

Titanite is a ubiquitous accessory mineral in metabasites in all zones. Individual titanite grains have an almost irregular habit. Titanite has a very close end-member composition ($CaTiSiO_5$).

Calcite occurs as a common metamorphic mineral in metabasites in zone I, and less commonly in zones II and III. In zones II and III calcite (with no inclusions) is a retrograde mineral, occurring in late veins. Aragonite was not identified. Hematite and magnetite occur as common but minor minerals in metabasites in all zones.

METAMORPHIC ASSEMBLAGES AND METAMORPHIC REACTIONS

The textural relationships and compositional data described above were used to determine the equilibrium assemblage for each metabasite. The equilibrium domain for a given assemblage was assumed to be about the size of a thin section. Representative assemblages for the three zones are presented in ACF diagrams in Fig. 9 [at fixed Fe/Mg and $Fe^{3+}/(Al + Fe^{3+})$ ratios] that effectively show; (i) the variation of assemblage as a function of bulk composition; and (ii) in zone III, the difference in composition between barroisite and crossite. The continuous and discontinuous reactions for the metamorphic zones were defined from these data.

The commonly observed assemblage of metabasites in zone I is Cal + Chl + Ep(+Ab + Qtz + Ttn + Ph + fluid). As shown in Fig. 9, the tie line of

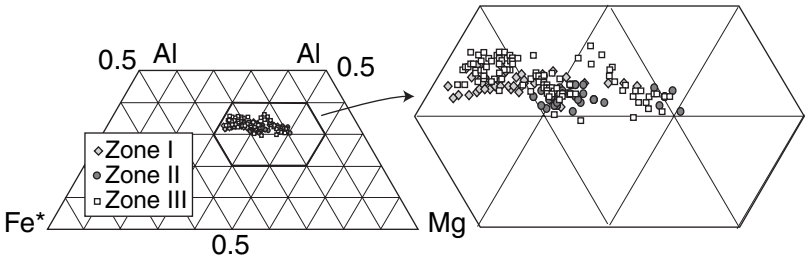

Fig. 8. Al-Fe*-Mg plot of chlorite to illustrate the effect of prograde and retrograde metamorphism and of bulk rock Fe/Mg ratio on chlorite composition.

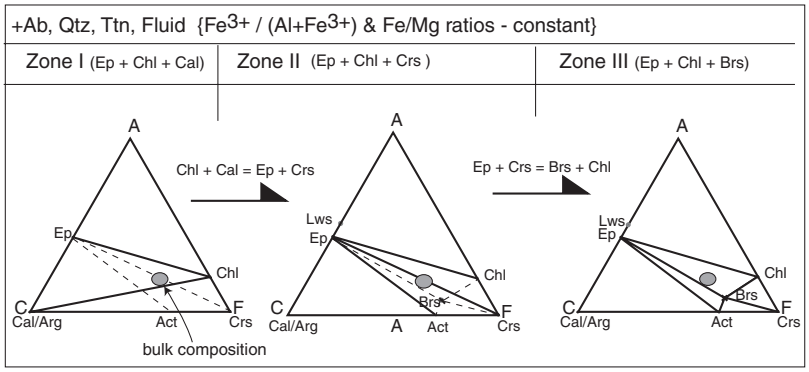

Fig. 9. $A(Al_2O_3 + Fe_2O_3\text{-}Na_2O\text{-}K_2O)$-$C(CaO)$-$F(FeO + MgO + MnO)$ diagrams showing the paragenetic relationships of amphibole and CaAl-silicates in three metamorphic zones. Excess phases are albite, quartz, titanite and H_2O-CO_2 fluid.

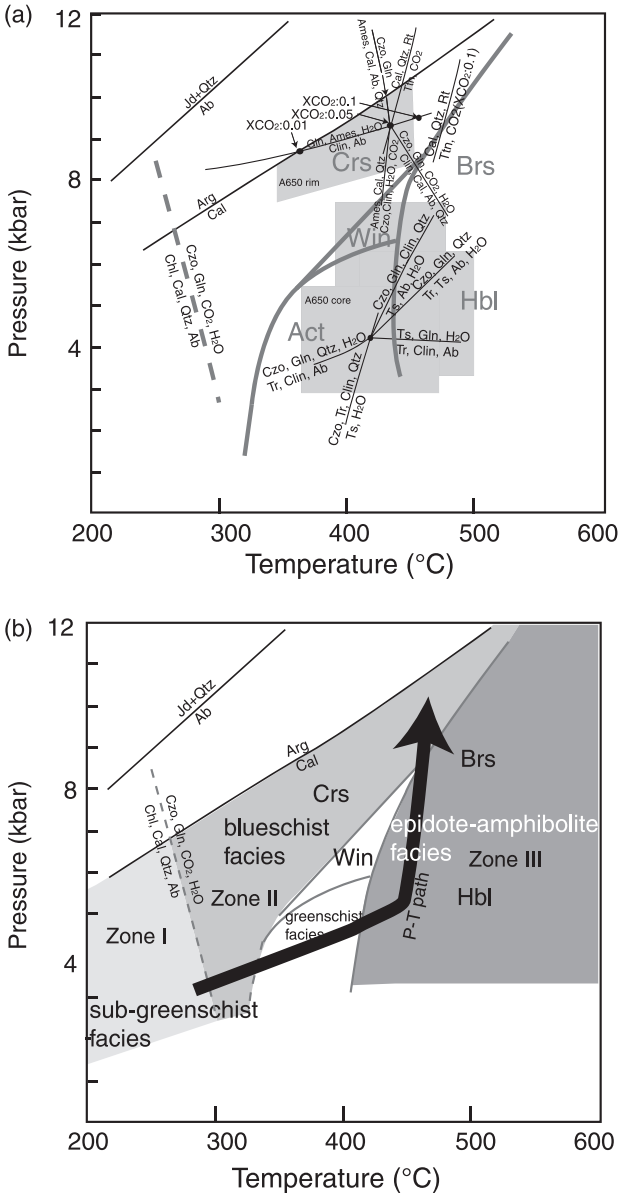

Fig. 10. (a) *P–T* trajectory of zoned amphibole in A650. Invariant points at 4.2 kbar/422 °C and 6.2 kbar/435 °C were calculated using core and mantle compositions of amphibole. *P–T* condition of rim composition constrained by the tie line of the invariant point of four reactions and decomposition reaction of titanite for different X_{CO_2}. Semi-quantitative phase relationships between Na-amphibole, winchite, actinolite and barroisite in basic schists are based on Otsuki & Banno (1990). Dotted line indicates the qualitative reaction Chl + Cal + Qtz + Ab = Czo + Crs + H_2O + CO_2; (b) *P–T* condition of each zone, facies series and *P–T*-time path are from this study.

Cal + Chl is stable and common metabasites contain the three-phase assemblage Cal + Chl + Ep together with excess phases. The maximum Al content of analysed epidote is smallest in zone I (Fig. 7). Generally, the Al content of epidote increases with metamorphic grade (Maruyama & Liou, 1988), indicating that the metamorphic grade is lowest in zone I. The muscovite components in phengite are smallest in zone I; this also suggests that the metamorphic-grade is lowest in zone I (Maruyama & Liou, 1988).

In zone II the most common assemblage of metabasites is Ep + Chl + Crs with excess phases. The tie line of Ep + Crs is stable. Metabasites in zone II are characterized by replacement of the join Cal-Chl by Ep-Crs. This relationship is described by the reaction Ab + Cal + Chl + Qtz = Crs + Ep + H_2O + CO_2. In zone III metabasites are characterized by the assemblage Ep + Chl + Brs and by replacement of the join Ep-Crs by Ep-Brs.

The mineral assemblage in each zone defines the relevant metamorphic facies: sub-greenschist (zone I), blueschist (zone II), albite-epidote amphibolite (zone III). Greenschist-facies assemblages are also present in zone II although minor. Overall, the metamorphic facies series belongs to the high-pressure intermediate type of Miyashiro (1965).

Mineral equilibria were calculated using THERMOCALC version 3.25 (Holland & Powell, 1998) in the Na_2O-CaO-MgO-Al_2O_3-SiO_2-H_2O system. The activities of end-members used in the *P–T* estimations were obtained using the AX program. Excess phases are quartz, albite and H_2O + CO_2 fluid.

Generally, zoning of Ca-Na amphibole is common in zone III, where barroisitic Ca-amphibole is rimmed by crossite (Figs 5a & 6); this suggests the dehydration reaction Gln + Ep + Qtz + fluid = Ab + Chl + Brs. The assemblage Gln + Brs + Chl + Ep + Ab + Qtz + fluid is related by the following five reactions using end-member activities:

$$6Tr + 9Clin + 50Ab = 25Gln + 6Czo + 7Qtz + 14H_2O \quad (1)$$

$$Tr + 2Clin + 8Ab = Ts + 4Gln + 4H_2O \quad (2)$$

$$14Gln + 12Czo + 14Qtz = 3Tr + 9Ts + 28Ab + 8H_2O \quad (3)$$

$$Gln + 3Clin + 6Czo = 6Ts + 2Ab + 10H_2O \quad (4)$$

$$Tr + 14Clin + 24Czo + 28Qtz = 25Ts + 44H_2O \quad (5)$$

These five reactions define an invariant point at 4.2 kbar/422 °C and 6.2 kbar/435 °C by using the core and mantle compositions of zoned amphibole of A650 in the NCMASH system. Furthermore, the *P–T* condition of the rim composition is defined by four reactions using end-member activities:

$$10Ab + 4Cal + 3Clin + 7Qtz = 5Gln + 2Czo + 6H_2O + 4CO_2 \quad (6)$$

$$8\mathrm{Ab} + 8\mathrm{Cal} + 3\mathrm{Ames} + 14\mathrm{Qtz} = 4\mathrm{Gln} + 4\mathrm{Czo} + 6\mathrm{H_2O} + 8\mathrm{CO_2} \quad (7)$$

$$5\mathrm{Ames} + 8\mathrm{Cal} + 14\mathrm{Qtz} = 4\mathrm{Clin} + 4\mathrm{Czo} + 2\mathrm{H_2O} + 8\mathrm{CO_2} \quad (8)$$

$$2\mathrm{Clin} + 4\mathrm{Ab} = 2\mathrm{Gln} + \mathrm{Ames} + 2\mathrm{H_2O} \quad (9)$$

These four reactions define an invariant point that shifts towards higher temperature with increasing $X\mathrm{CO_2}$. The decomposition reaction of titanite to rutile for different $X\mathrm{CO_2}$ constrains the maximum $X\mathrm{CO_2}$ (0.05). The tie line of these invariant points with different $X\mathrm{CO_2}$ (approximately 0.05) effectively indicates the pressure condition of that mineral assemblage (Fig. 10a).

The equilibrium conditions of zoned amphibole are used to define the *P–T* trajectory for metabasites in zone III (Fig. 10b). To delineate the *P–T* condition for each zone and the *P–T*-time path, the most diagnostic mineral and mineral composition is Ca-Na amphibole. For the buffered assemblage, the stability field of amphibole is generally shown in Fig. 10b (Otsuki & Banno, 1990). Glaucophane is stable on the higher-*P* side at a wide range of temperature (300–500 °C), whereas actinolite-hornblende is stable on the lower-*P* side for the same temperature range of glaucophane. In-between, winchite is stable at lower-*T* and barroisite at higher-*T* (Fig. 10b).

The mineral assemblages in zones, I, II and III, and the amphibole compositional change with increasing metamorphism were used to define the anticlockwise *P–T* path and *P–T*-time path shown in Fig. 10b.

DISCUSSION

The Anglesey blueschist belt was well defined by the classic mapping of Greenly (1919). After this pioneering work, few modern mineralogical studies have been undertaken on these high-pressure rocks (Gibbons & Mann, 1983; Gibbons & Gyopari, 1986; Horák & Gibbons, 1986). Some blueschist belts in circum-Pacific subduction-accretion complexes and orogenic belts such as Japan have similar mineral zones and geological setting as those on Anglesey and, we suggest, provide a background and modern analogue for interpretation of the Anglesy rocks (Ota *et al.*, 2004 for the Sanbagawa belt; Sakakibara & Ota, 1994 for the Kamuikotan belt).

This study of the mineral zones, mineral assemblages and mineral compositions indicates a subduction zone geotherm that ranged from 15 °C km^{-1} (300 °C) to 35 °C km^{-1} (500 °C), following a high-pressure intermediate metamorphic facies series similar to that of the Cretaceous Sanbagawa belt, Japan (Miyashiro, 1965, 1994). The *P–T*-time path and metamorphic facies series indicate an anticlockwise evolution (see also Gibbons & Gyopari, 1986) that is consistent with the calculated geothermal gradient along a Benioff zone (e.g. Peacock, 2001). Recent well-documented analyses of the *P–T* trajectory and metamorphic facies series of comparable blueschist belts support an anticlockwise, rather than a classic clockwise path (Aoya *et al.*, 2003; Ota *et al.*, 2004 for Sanbagawa, Japan). Although not in the circum-Pacific, the Kokchetav diamond-coesite-bearing rocks in Kazakhstan have a similar anticlockwise *P–T*-path (Omori & Masago, 2004).

The Anglesey blueschist belt is a small piece of an accretionary orogen. Both the Sanbagawa (Isozaki & Itaya, 1991) and Franciscan blueschist belts (Kimura

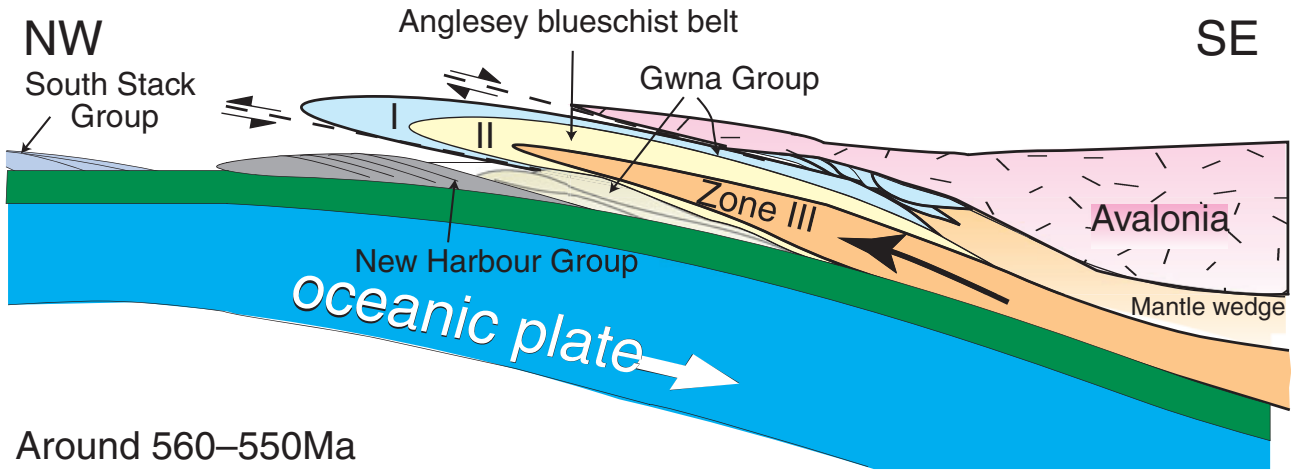

Fig. 11. Simplified cross-sections along a NW-SE profile through Anglesey to illustrate the geodynamic evolution of the active western margin of Avalonia during the exhumation of the Anglesey blueschist belt at *c.* 570–550 Ma. A thin ductile wedge of the subduction-accretion complex was recrystallized under blueschist facies conditions, and transported to a mid-crustal level. The central high-pressure zone is flanked by lower grade zones in an isoclinal antiform. In the northwest of this accretionary orogen pasive margin quartzites of the youngest South Stack Group were the last rocks to be accreted by underplating towards the southeast beneath the New Harbour Group (see text for further discussion).

et al., 1996), which may be regarded as representative world-standards of high-pressure rocks in accretionary orogens, occur as thin (<1 km), flat-lying tectonic slices cut on the top and bottom by normal and reverse faults respectively. The shallow subhorizontal structure, size and thickness of the Anglesey blueschist belt and the range of metamorphic grade from subgreenschist through blueschist to epidote-amphibolite facies, all demonstrate that this is a typical blueschist belt.

Horák *et al*. (1996) pointed out that a calcalkaline magmatic arc crops out in the Snowdon Mountains to the east of the blueschist belt, which they envisaged was created by the eastward subduction of the Anglesey rocks. Accordingly, the subduction zone should have been located between the arc and the blueschists near the present-day Menai Strait fault. It is interesting to note in passing that the section across Anglesey is very similar to the Cenozoic trench-arc section across Japan with the Ryukyu arc on the west side of the fault of the Median Tectonic Line (Maruyama *et al*., 1997).

The tectonic belts and metamorphic zones on Anglesey have a symmetrical arrangement (Figs 1, 2 & 3). The map of the British Geological Survey (1980) shows that the central high-pressure 'Penmynydd metamorphic zone' with blueschists and mica schists (zone III; Fig. 3) is bordered on both sides by Gwna Group belts that contain lower grade greenschists, spilitic lavas and albite diabases (zone I; Fig. 3). The western half of the eastern Gwna belt shows evidence of blueschist metamorphism (zone II; Fig. 3). Such an arrangement of metamorphic belts and zones with the highest pressure and deepest rocks in the centre and flanked by lower grade rocks on either side suggests an antiformal structure. We note that a similar arrangement of metamorphic zones and antiformal structure is common to the high-pressure Sanbagawa belt of Japan (Ota *et al*., 2004) and the ultrahigh-pressure Kokchetav belt in Kazakhstan (Kaneko *et al*., 2000). It is suggested that the metamorphic zones in Anglesey have an isoclinal structure, as depicted in Fig. 11. Accordingly, this is an example of wedge extrusion at an accretionary plate boundary (Ernst *et al*., 1997). Our model for the east-dipping metamorphic zones is compatible with their position in a southeast-dipping accretionary orogen, The tectonic model of the accretionary orogen depicted in Fig. 11 is consistent with the fact that the last rocks to be underplated in the west were passive margin sediments (mostly quartzite) of the South Stack Group that contain zircon with the youngest age of 501 $\pm$ 10 Ma in Anglesey (Collins & Buchan, 2004).

ACKNOWLEDGEMENTS

We are deeply indebted to Drs A. Collins, T. Tsujimori, van Staal and Prof. M. Brown for their critical reviews and constructive comments. We thank Dr M. Wood for useful information and discussions on the geology of Anglesey, Drs S. Omori, T. Ota, T. Komiya and K. Kitajima for their helpful advice and R. Hanada for encouragement.

REFERENCES

Aoya, M., Uehara, S., Matsumoto, M., Wallis, S. R. & Enami, M., 2003. Subduction-stage pressure-temperature path of eclogite from the Sambagawa belt: prophetic record for oceanic-ridge subduction. *Geology*, **31,** 1045–1048.

Barber, A. J. & Max, M. D., 1979. *A New Look at the Mona Complex, Anglesey, North Wales*. Journal of the Geological Society, London, **136,** 407–432.

Blake, J. F., 1888. The occurrence of glaucophane-bearing rocks in Anglesey. *Geological Magazine*, **5,** 125–127.

British Geological Survey, 1980. *1:50,000 Geological Map of Anglesey*, Special Sheet, Solid with Drift edition.

Carman, J. H. & Gilbert, M. C., 1983. Experimental studies on glaucophane stability. *American Journal of Science*, **283,** A, 414–437.

Collins, A. S. & Buchan, C., 2004. Provenance and age constraints of the South Stack Group, Anglesey, UK: U-Pb SIMS detrital zircon data. *Journal of the Geological Society, London*, **161,** 743–746.

Dallmeyer, R. D. & Gibbons, W., 1987. The age of blueschist metamorphism on Anglesey, North Wales: evidence from $^{40}Ar/^{39}Ar$ mineral dates of the Penmynydd schists. *Journal of the Geological Society, London*, **144,** 843–850.

Ernst, W. G., 1963. Polymorphism in alkali amphiboles. *American Mineralogist*, **48,** 1357–1373.

Ernst, W. G., Maruyama, S. & Wallis, S., 1997. Buoyancy-driven, rapid exhumation of ultrahighpressure metamorphosed continental crust. *Proceedings of the National Academy of Science*, **94,** 9532–9537.

Gibbons, W., 1983. Stratigraphy, subduction and strike-slip faulting in the Mona Complex of North Wales – a review. *Proceeding of the Geologists' Association*, **94,** 147–163.

Gibbons, W., 1989. Suspect terrane definition in Anglesey, North Wales. *Geological Society of America, Special Papers*, **23,** 59–65.

Gibbons, W. & Gyopari, M., 1986. A greenschist protolith for blueschists on Anglesey, U.K. In: *Blueschists and Eclogites*, (eds Evans, B. W. & Brown, E. H.), *Geological Society of America. Memoir*, **164,** 217–228.

Gibbons, W. & Horák, J., 1990. Contrasting metamorphic terranes in northwest Wales. In: *The Cadomian Orogeny* (eds D'Lemos, R. S., Strachan, R. A. & Topley, C. G.), *Geological Society, London, Special Publication*, **51,** 315–327.

Gibbons, W. & Mann, A., 1983. Pre-Mesozoic lawsonite in Anglesey, northern Wales: preservation of ancient blueschists. *Geology*, **11,** 3–6.

Greenly, E., 1919. *The Geology of Anglesey, Memoir Geological Survey of Great Britain*. (2 vols.). HMSO, London, 980 pp.

Henslow, J. S., 1822. Geological description of Anglesea. *Transactions of the Cambridge Philiosophical Society*, **1,** 359–452.

Holland, T. J. B. & Blundy, J., 1994. Non-ideal intersections in calcic amphiboles and their bearing on amphibole-plagioclase thermometry. *Contributions to Mineralogy and Petrology*, **116,** 433–447.

Holland, T. J. B. & Powell, R., 1998. An internally consistent thermodynamic data set for phases of petrological interest. *Journal of Metamorphic Geology*, **16,** 309–343.

Horák, J. M. & Gibbons, W., 1986. Reclassification of blueschist amphiboles from Anglesey, North Wales. *Mineralogical Magazine*, **50,** 533–535.

Horák, J. M., Doig, R., Evans, J. A. & Gibbons, W., 1996. Avalonian magmatism and terrane linkage: new isotopic data from the Precambrian of North Wales. *Journal of the Geological Society of London*, **153,** 91–99.

Isozaki, Y. & Itaya, T., 1991. Pre-Jurassic klippe in northern Chichibu belt in west-central Shikoku, Southwest Japan-Kurosegawa terrane as a tectonic outlier of the pre-Jurassic rocks of the Inner Zone. *Journal of the Geological Society of Japan*, **97,** 431–450.

Kaneko, Y., Terabayashi, M., Katayama, I. *et al*., 2000. Geology of the Kokchetav UHP-HP massif Kazakhstan central Asia. *The Island Arc*, **9,** 264–283.

Kimura, G., Maruyama, S., Isozaki, Y. & Terabayashi, M., 1996. Well-preserved underplating structure of the jadeitized Franciscan complex. Pacheco Pass. *California. Geology*, **24,** 75–78.

Kretz, R., 1983. Symbols for rock forming minerals. *American Mineralogist*, **68,** 277–279.

Leake, B. F., Woolley, A. R., Arps, C. E. S. *et al*., 1997. Nomenclature of amphiboles: report of the subcommittee on amphiboles of the International Mineralogical Association, commission on new minerals and mineral names. *American Mineralogist*, **82,** 1019–1037.

Liou, J. G. & Maruyama, S., 1987. Parageneses and compositions of amphiboles from Franciscan jadeite-glaucophane type facies series metabasites at Cazadero, California. *Journal of Metamorphic Geology*, **5,** 371–395.

Maruyama, S. & Liou, J. G., 1988. Petrology of Franciscan metabasites along the jadeite-glaucophane type facies series, Cazadero, California. *Journal of Petrology*, **29,** 1–37.

Maruyama, S., Liou, J. G. & Terabayashi, M., 1996. Blueschists and eclogites of the world and their exhumation. *International Geology Review*, **38,** 485–594.

Maruyama, S., Isozaki, y., Kimura, G. & Terabayashi, M., 1997. Paleogeographic maps of the Japanese Islands: plate tectonic synthesis from 750 Ma to the present. *The Island Arc*, **6,** 121–142.

Matsumoto, M., Wallis, S., Aoya, M., Enami, M., Kawano, J. & Seto, Y., 2003. Petrological constraints on the formation conditions and retrograde P-T path of the Kotsu eclogite unit, central Shikoku. *Journal of Metamorphic Geology*, **21,** 363–376.

Miyashiro, A., 1957. The chemistry, optics and genesis of the alkali-amphiboles. *Journal of Faculty of Science, University of Tokyo*, Sect.2 **11,** 57–83.

Miyashiro, A., 1965. *Metamorphic Rocks and Metamorphic Belts (in Japanese)*. pp. 458 Tokyo: Iwanami-Shoten.

Miyashiro, A., 1994. *Metamorphism (in Japanese)*. pp. 256, Tokyo: Iwanami-Shoten.

Omori, S. & Masago, H., 2004. Application of thermodynamic forward-modeling to estimate of a Metamorphic *P–T* path. *Journal of Geography*, **113,** 647–663.

Ota, T., Terabayashi, M. & Katayama, I., 2004. Thermobaric structure and metamorphic evolution of the Iratsu eclogite body in the Sanbagawa belt, central Shikoku, Japan. *Lithos*, **73,** 95–126.

Otsuki, M. & Banno, S., 1990. Prograde and retrograde metamorphism of hematite-bearing basic schists in the Sanbagawa belt in central Shikoku. *Journal of Metamorphic Geology*, **8,** 425–439.

Peacock, S. M., 2001. Are the lower planes of double seismic zones caused by serpentine dephdration in subducting oceanic mantle? *Geology*, **29,** 299–302.

Sakakibara, M. & Ota, T., 1994. Metamorphic evolution of the Kamuikotan high-pressure and low-temperature metamorphic rocks in central Hokkaido, Japan. *Journal of Geophysical Research*, **99,** B11, 22,221–22,235.

Shackleton, R. M., 1969. The Precambrian of North Wales. In: *The Precambrian and Lower Palaeozoic Rocks of Wales* (ed. Wood, A.), pp. 1–18, University of Wales Press, Cardiff.

Shackleton, R. M., 1975. Precambrian rocks of Wales. In: *A Correlation of Precambrian Rocks in the British Isles*. (ed. Harris, A. L.), Geological Society, London, Special Publications, **6,** 76–82.

Thorpe, R. S., 1993. Geochemistry and eruptive environment of metavolcanic rocks from the Mona complex of Anglesey, North Wales, U.K. *Geological Magazine*, **130,** 85–91.

Wood, D. S., 1974. In: *Ophiolites, mélanges, blueschists, and ignimbrites: early Caledonian subduction in Wales? Modern and Ancient Geosynclinal Sedimentation* (eds Dott, R. H. & Shaver, R. H.), *Society of Economic Paleontologists and Mineralogists, Special Publication*, **19,** 334–344.

Received 16 December 2005; revision accepted 19 June 2006.